Resonance behaviour of railway embankments on soft subsoil

Sulongge Gong [1,*], *Li* Wang[1], *Chen* Shen[1], *Cristina* Jommi [2,3], and *Zili* Li[1]

[1] Department of Engineering Structures, Delft University of Technology, Delft, The Netherlands
[2] Department of Geoscience and Engineering, Delft University of Technology, Delft, The Netherlands
[3] Department of Civil and Environmental Engineering, Politecnico di Milano, Milano, Italy

Abstract. Railway track on a layered substructure, such as an embankment-subsoil system, may exhibit subgrade resonance, and the influence of soft subsoil on the resonance is not yet fully understood. The present study investigates the subgrade resonance behaviour using falling weight tests at two sites in the Netherlands, supported by three-dimensional finite element modelling. The two sites have similar geometrical and material properties of track and embankment, but different subsoil conditions: sand at one site and peat at the other. The field measurements show clear amplification at about 25 Hz at the sandy site, whereas no distinct peak is observed at the peaty site. The measured resonance frequency at the sandy site can be reproduced with reasonable accuracy by a finite element model calibrated on field and literature data. The model is further used in a parametric study, which confirms that decreasing subsoil stiffness reduces the peak of the subgrade resonance. Experimental and numerical results demonstrate the effects of the embankment-subsoil impedance contrast on the dynamic behaviour of railway embankments: a soft-on-stiff configuration may lead to resonance, whereas a stiff-on-soft configuration results in a less pronounced resonant response.

1 Introduction

In the Netherlands, an extensive railway network operates over areas with highly compressible soft soils [1], such as peat. The railway infrastructure on soft subsoil presents engineering challenges, as soft soils are prone to excessive settlement and to dynamic amplification problems. For example, the critical speed phenomenon, which is a sonic-boom-like effect, occurs as the train speed approaches the surface wave speed of the substructure [2, 3].

Another resonance mechanism, and the focus of the present study, is subgrade resonance, which can be found for railway tracks on layered subgrade even when the train speed is well below the critical speed. The frequency associated with subgrade resonance is usually reported to be below 50 Hz [4–7]. Such resonance has practical implications, as dynamic amplification may occur when the resonant frequency coincides with relevant frequency components of the train loading, including the axle-passing frequency [8].

To investigate the resonance response of the railway track structure, hammer tests are commonly performed [9, 10], in which the structure is excited with an impact load and the receptance can be obtained. This approach has been used to characterise the properties of individual track components: Oregui et al. [11] identified characteristic frequency bands of damaged rails, demonstrating the sensitivity of receptance to rail surface condition; Maes et al. [12] measured the frequency- and the load - dependent dynamic stiffness and damping of rail pads; Kaewunruen [13] evaluated the natural frequencies and damping of prestressed concrete sleepers under different support conditions; Liu et al. [14] studied the vertical vibration and transmission characteristics of railway ballast under impact loading, highlighting the role of ballast damping in vibration propagation.

Nevertheless, hammer tests are usually not able to capture the influence of the subgrade, due to the relatively low excitation energy and the strong damping in the subgrade layers [15]. The influence of substructure properties on receptance behaviour is thus often studied using numerical or analytical models [4, 5]. Experimental study remains limited, particularly for sites with soft subsoil.

In the present study, falling weight tests are used to investigate the subgrade resonance, which enables more effective excitation of the railway subgrade due to the higher impact load with magnitudes comparable to those induced by operational trains [16]. Two sites with distinctive subsoil conditions are investigated: at one site, the embankment is founded on stiff sandy subsoil, while at the other it rests on soft organic subsoil. The comparison between the two sites allows assessing the influence of subsoil stiffness on the resonance characteristics. A three-dimensional finite element model is set up to reproduce the falling weight impact tests. A parametric study is performed to further investigate the influence of subsoil stiffness on the resonance behaviour.

* Corresponding author: l.su-1@tudelft.nl

2 Falling weight test on railway tracks

2.1 Test setup and site conditions

The test uses an equipment [15,16] that can release stacked weights from a specified height, as shown in Fig. 1.

Fig. 1. Overview of the falling weight impact test equipment on the railway track.

A load cell is integrated into the plastic tip of the falling weight to measure the impact force. During testing, stacked weights of 100 kg are dropped from a height of 40 cm onto the railhead. To measure the response of the system, accelerometers are installed at the railhead, sleeper, ballast, and along the inspection path at 2 m and 4 m from the track centreline. The measurement points are denoted as R0, S0, B0, Y2, and Y4, respectively. Excitation force and acceleration are recorded and synchronised using a data acquisition system. The resonance behaviour of the track is then examined using the transfer function between the displacement and the impact force. In particular, the receptance function is defined as in Eq.(1):

$$H_{wF}(f) = \frac{S_{wF}(f)}{S_{FF}(f)} \quad (1)$$

where $S_{wF}(f)$ is the cross-spectrum of the force and displacement, and $S_{FF}(f)$ is the autospectrum of the force.

Falling weight tests were conducted at two sites in the Netherlands. A general schematic of the cross-sectional profile of the railway embankment and subsoil of the two sites is shown in Fig. 2.

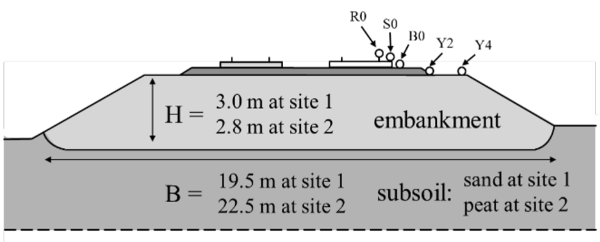

Fig. 2. Schematisation of the simplified cross-sectional profile of the railway embankment at the two sites and sensor positions.

Although the two sites have similar embankment geometry and properties, they differ significantly as for subsoil conditions. Site 1, located on the Tilburg-Boxtel railway line, consists primarily of sandy subsoil, whereas Site 2, located on the Delft-Schiedam line, consists of peat down to a depth of approximately 8 m, as indicated in the cone penetration test (CPT) results shown in Fig. 3. The water tables are located 0.4 m and 0.6 m below the ground level at the polder side at site 1 and site 2, respectively.

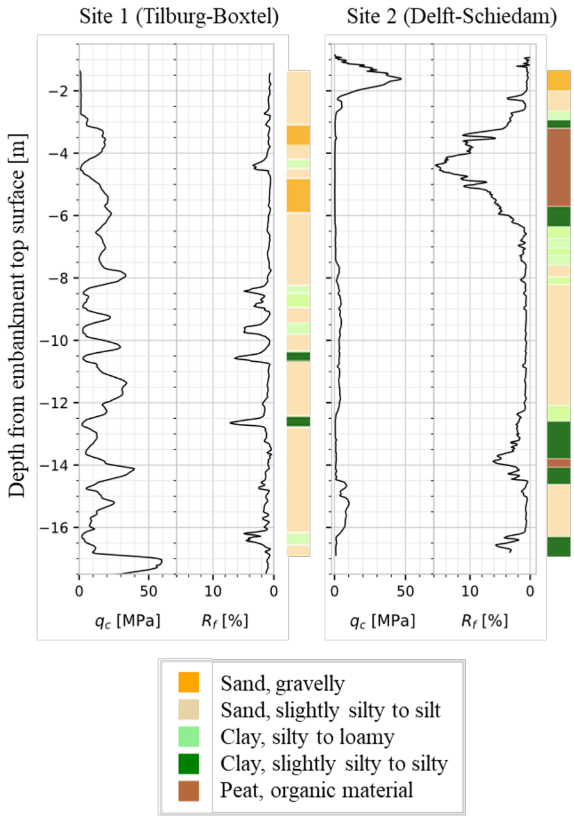

Fig. 3. Cone penetration test result at two sites: cone resistance q_c, friction ratio R_f, and soil classification.

The shear wave velocity profiles were measured using seismic cone penetration tests (SCPT) [17] at site 1 and using multichannel analysis of surface waves test (MASW) [18] at site 2. The measured shear wave velocity and the corresponding elastic moduli representative for embankment and subsoil at the two sites are summarised in Table 1.

Table 1. Measured elastic properties at two sites.

	embankment		subsoil	
	v_s [m/s]	E [MPa]	v_s [m/s]	E [MPa]
Site 1	173	145	200	216
Site 2	165	132	85	39

2.2 Experimental results

The direct receptance measured at the railhead (R0) for the tests conducted at the two sites are shown in Fig. 4. At site 1, a peak is visible around 25 Hz, corresponding to the anticipated resonance frequency range of the railway subgrade. The frequency associated with this peak is hereafter referred to as the subgrade resonance frequency. In the present configuration, where the embankment forms the uppermost layer of the substructure, this frequency can be equivalently referred to as embankment resonance frequency. Unlike site 1, site 2 shows no clear peak at the lower end of the frequency range (below 50 Hz). Peaks at high frequencies (greater than 100 Hz) have been observed, which are expected to be associated with properties of track components above the embankment [10].

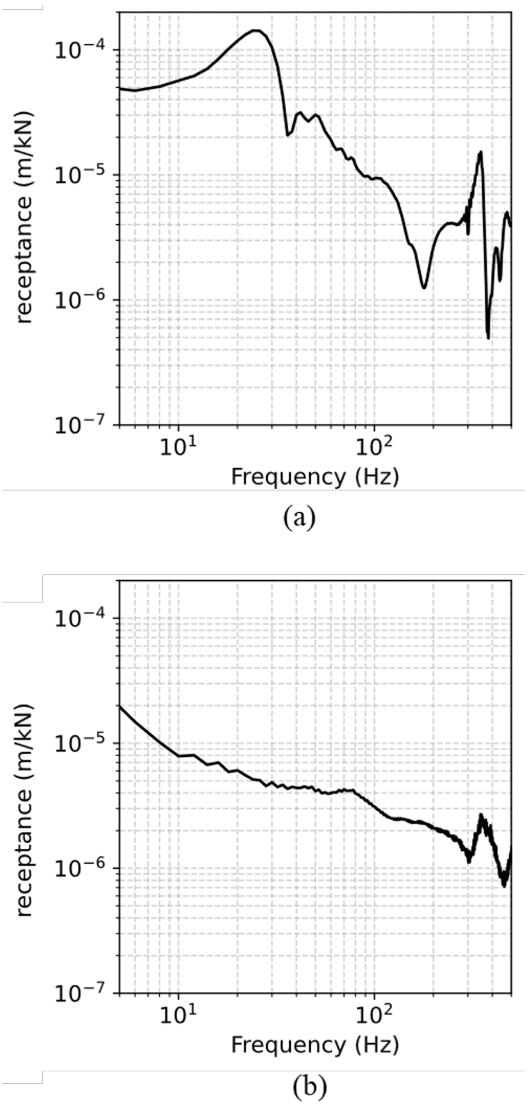

Fig. 4. Receptance measured at impact location for two sites: (a) Site 1: Tilburg-Boxtel and (b) Site 2: Delft-Schiedam.

To further study the pattern of receptance in the low-frequency range, the direct and cross receptance measured at two sites are plotted in Fig. 5. At site 1, the 25 Hz peaks are observed in the receptance across all measured locations, whereas at site 2, no distinct peak can be seen in direct and cross receptance.

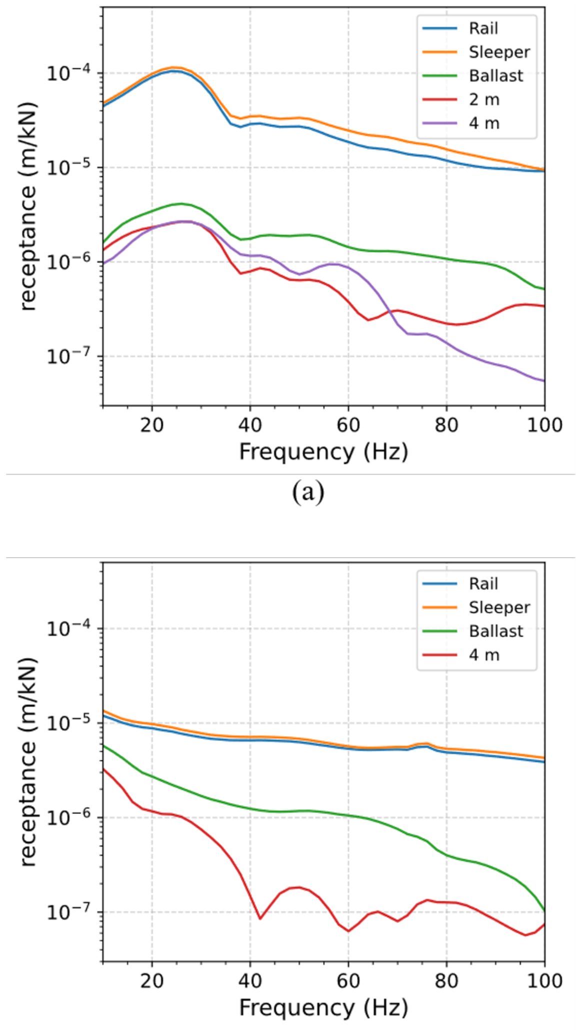

Fig. 5. Direct and cross receptance for two sites: (a) Site 1: Tilburg-Boxtel, and (b) Site 2: Delft-Schiedam.

3 Numerical modelling

3.1 FE model setup

A three-dimensional finite element model with explicit time integration was developed in software ANSYS/LS-DYNA to simulate the falling weight test conducted at site 1 (Tilburg-Boxtel site), as shown in Fig. 6.

The model incorporates the major components of the railway track (rails, fasteners, sleepers, and ballast), the embankment, and the subsoil. The UIC54 rails are modelled using Timoshenko beam elements, and the fasteners are modelled with spring and damper elements. All other components are modelled with 8-node reduced-integration solid elements, and a stiffness form of Flanagan-Belytschko hourglass control [24] is used for solid elements. The interactions between the NS90 sleeper and ballast, and between the ballast and embankment, are modelled as tied contacts using penalty-based algorithm. The saturated subsoil is treated as an incompressible single-phase medium.

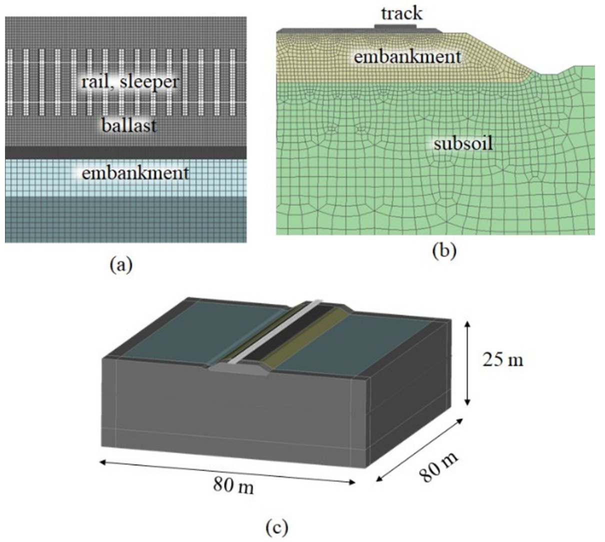

Fig. 6. Numerical model of the track-embankment-subsoil system: (a) plan view of the track structure; (b) cross-sectional view; (c) model dimension.

The material properties used in the model are listed in Table 2. To account for material damping, stiffness-proportional damping is introduced for the embankment and the subsoil [25]. Damping ratios of 2% and 5% are adopted for the embankment and sand layers, respectively, based on typical values and then calibrated against the experimental results. The stiffness and damping coefficient of the fastener are defined as 1200 MN/m and 70 kN/(m/s).

The model has a horizontal dimension of 80×80 meters and a height of 25 meters. To avoid spurious reflection at the model boundary, absorbing boundary condition are applied by placing perfectly-matched layer (PML) [19] at the outer boundaries. The time step is 5.3×10^{-6} s, which satisfies the Courant stability criterion and is governed by the beam elements of 0.1 meter in the rails.

To simulate the falling weight test, the time history of the impact force measured during the field test is used as input and applied to the rail as a concentrated load. The accelerations are collected at locations corresponding to the measurement points, and receptance can then be calculated.

Table 2. Material properties adopted in the model.

Material	ρ [kg/m^3]	E [MPa]	ν [-]
Rail (UIC54)	7850	210×10^3	0.3
Sleeper (NS90)	2520	38.4×10^3	0.2
Ballast	1800	70	0.25
Embankment	1800	150	0.3
Subsoil	2000	250	0.49

3.2 Model validation

Fig. 7 compares the simulated and measured receptance, normalized by their respective amplitude at 10 Hz, at various locations at site 1.

As shown in Fig. 7, the resonant peak around 25 Hz is well captured at all measurement locations. The model is therefore used for further analysis on subgrade resonance.

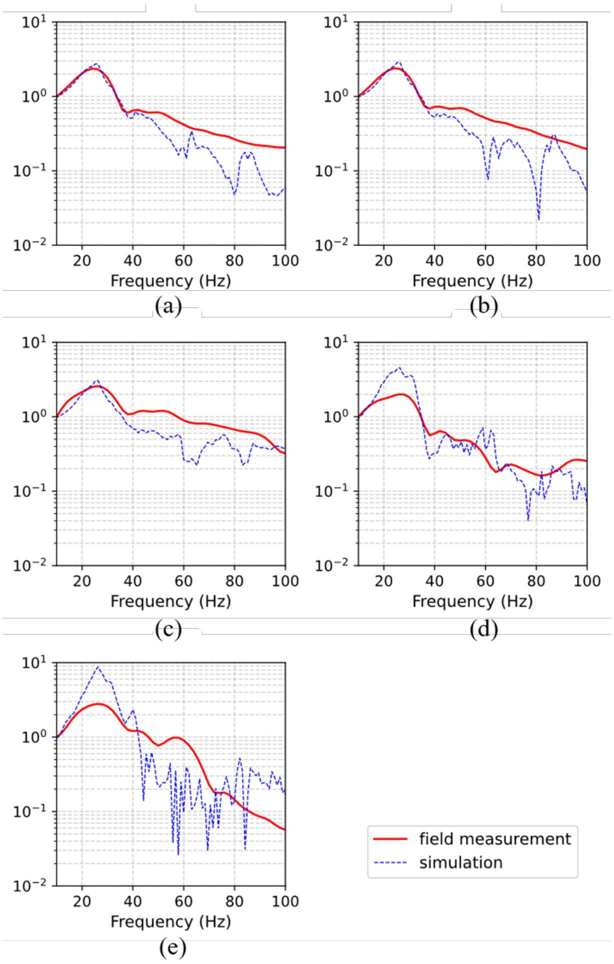

Fig. 7. Normalized receptance in field measurement and simulation at various positions: (a) R0; (b) S0; (c) B0; (d)Y2; (e)Y4.

4 Discussion

From the receptance measured at the two sites, two main features can be identified. First, a peak at around 25 Hz is observed at site 1, which is anticipated to be associated with the railway subgrade.

The subgrade resonant frequency is commonly calculated by referring to the fundamental compression mode for an elastic layer resting on a stiff foundation [20–24]. The fundamental frequency is defined in Eq.(2), where c_p is the compression wave velocity of the layer, and H is the layer thickness, which equals a quarter wavelength of the fundamental mode:

$$f_0 = \frac{c_p}{4H} \tag{2}$$

Auersch [7] proposed an alternative expression (Eq.(3)) based on the characteristics of Rayleigh wave propagation in layered soil, where c_R is the Rayleigh wave velocity.

$$f_0 = \frac{c_R}{2H} \quad (3)$$

Considering the embankment thickness of $H = 3$ m, the embankment shear wave velocity c_s = 180 m/s measured in the SCPT test, and a Poisson's ratio of 0.3, the subgrade resonance frequency f_0 is equal to 27.9 Hz and 27.6 Hz using Eq.(2) and Eq.(3), respectively. These values are close to the resonant frequency measured at site 1.

The second observation is that the receptance measured at site 2 shows no distinct peak below 50 Hz, which suggests a strongly damped behaviour and, consequently, a less noticeable, possibly diminished, subgrade resonance peak.

In this sense, higher material damping of the subsoil material at site 2 certainly plays a role. Still, a stiff-on-soft soil layering can also result in higher radiation damping [7, 20], meaning more energy is dissipated into the subsoil, contrary to the situation at site 1 with the soft-on-stiff soil layering, where more energy is reflected and trapped in the relatively softer upper embankment layer. Besides, the change from a soft-on-stiff to a stiff-on-soft subgrade will affect the phase of the reflected wave, which can result in destructive interference at the top surface resulting in a lower receptance amplitude.

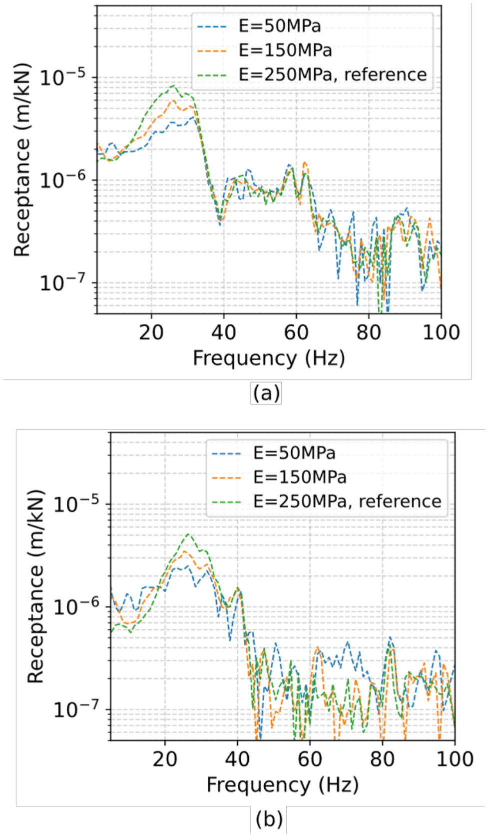

Fig. 8. Influence of subsoil stiffness on receptance measured on the embankment top surface at location: (a) Y2 and (b) Y4.

It is noted that, although the two sites have broadly similar embankment properties, the embankment properties are not identical, as shown in Figure 2 and Table 1. Therefore, the comparison of experimental receptance between the two sites is focused on qualitative feature, which is the presence of the resonance peak, rather than on quantitative differences in receptance amplitude.

To numerically assess the effect of subsoil stiffness, a parametric study is conducted. The Young's modulus of the subsoil is taken as 50, 150, and 250 MPa (reference case). The results are presented for the receptance measured on the embankment top surface at locations Y2 and Y4.

Fig. 8 shows the effect of subsoil stiffness on the simulated receptance. As the subsoil stiffness decreases, the resonant peak around $c_p/4H$ decreases on the embankment surface, with the lowest amplitude in the low frequency range found for the softest subsoil. Overall, the results of the parametric study are consistent with the observations at two sites.

5 Conclusion

The present study investigates the resonance behaviour of railway embankments through falling weight tests and finite element simulations. The measurements revealed a vertical amplification peak at about 25 Hz at the site with sandy subsoil, whereas no distinct peak was observed at this range at the peat site.

The FE model of the falling weight test captures the resonance frequency at the sandy site with reasonable accuracy, and the parametric study shows that reducing subsoil stiffness lowers the amplitude at the resonance frequency. The different resonance behaviour can be explained by the impedance contrast between the embankment and the underlying soil: a soft-on-stiff subgrade layering promotes a subgrade resonance around $c_p/4H$, whereas a stiff-on-soft configuration results in a less pronounced resonant response.

Overall, the experimental findings confirm the capability of the falling weight test to measure subgrade resonance and, together with numerical modelling, provide insight into the influence of soft subsoil on the resonance behaviour of railway embankment.

The financial support of ProRail, under the project "RESET: Reliable Embankments for Safe Expansion in Rail Traffic", is gratefully acknowledged.

References

1. A. A. Balkema. Building on Soft Soils: Design and construction of earth structures both on and into highly compressible subsoils of low bearing capacity. (Routledge, Rotterdam, 1996)
2. C. Madshus, A.M. Kaynia. High-speed railway lines on soft ground: dynamic behaviour at critical train speed. J. Sound Vib. **231**, 689–701 (2000). https://doi.org/10.1006/JSVI.1999.2647
3. V.V. Krylov. Generation of ground vibrations by superfast trains. Appl. Acoust. **44**, 149–164 (1995). https://doi.org/10.1016/0003682X(95)91370-I
4. A.C. Lamprea-Pineda, D.P. Connolly, A. Castanheira-Pinto, et al. On railway track receptance. Soil Dyn. Earthquake Eng. **177**, 108331 (2024). https://doi.org/10.1016/j.soildyn.2023.108331

5. J.Y. Shih, D.J. Thompson, E. Ntotsios. Analysis of resonance effect for a railway track on a layered ground. Transp. Geotech. **16**, 51–62 (2018). https://doi.org/10.1016/j.trgeo.2018.07.001
6. E. Arlaud, S. Costa D'Aguiar, E. Balmes. Receptance of railway tracks at low frequency: numerical and experimental approaches. Transp. Geotech. **9**, 1–16 (2016). https://doi.org/10.1016/j.trgeo.2016.06.003
7. L. Auersch. Wave Propagation in Layered Soils: Theoretical Solution in Wavenumber Domain and Experimental Results of Hammer and Railway Traffic Excitation. J. Sound Vib. **173**, 233–264 (1994). https://doi.org/10.1006/jsvi.1994.1228
8. D.P. Connolly, P.A. Costa. Geodynamics of very high speed transport systems. Soil Dyn. Earthquake Eng. **130**, 105982 (2020). https://doi.org/10.1016/j.soildyn.2019.105982
9. K. Knothe, Y. Wu. Receptance behaviour of railway track and subgrade. Arch. Appl. Mech. (Ing. Arch.) **68**, 457–470 (1998). https://doi.org/10.1007/s004190050179
10. A.P. De Man. Dynatrack: A survey of dynamic railway track properties and their quality. Ph.D. thesis, Delft University of Technology (2002)
11. M. Oregui, Z. Li, R. Dollevoet. Identification of characteristic frequencies of damaged railway tracks using field hammer test measurements. Mech. Syst. Signal Process. **54**, 224–242 (2015). https://doi.org/10.1016/j.ymssp.2014.08.024
12. J. Maes, H. Sol, P. Guillaume. Measurements of the dynamic railpad properties. J. Sound Vib. **293**, 557–565 (2006). https://doi.org/10.1016/j.jsv.2005.08.042
13. S. Kaewunruen. Experimental and numerical studies for evaluating dynamic behaviour of pre-stressed concrete sleepers subject to severe impact loading. J. Proc. R. Soc. N.S.W. **141**, 52–53 (2008). https://doi.org/10.5962/p.361619
14. G. Liu, J. Cong, P. Wang, et al. Study on vertical vibration and transmission characteristics of railway ballast using impact hammer test. Constr. Build. Mater. **316**, 125898 (2022). https://doi.org/10.1016/j.conbuildmat.2021.125898
15. S. Unsiwilai. Railway track support condition assessment: from onboard measurement to maintenance decision support. Ph.D. thesis, Delft University of Technology (2024)
16. S. Unsiwilai, C. Shen, Y. Zeng, et al. Vertical dynamic measurements of a railway transition zone: a case study in Sweden. J. Civ. Struct. Health Monit. **14**, 979–996 (2024). https://doi.org/10.1007/s13349-024-00766-0
17. O. Winkel, C. van Isselt, O. Duizendstra. Report seismic CPT investigation Oisterwijk. (Fugro, Leidschendam, 2025)
18. S. Elgun, C. van Isselt, Report MASW measurements Delft Campus-Schiedam (Fugro, Leidschendam, 2023)
19. U. Basu, A.K. Chopra. Perfectly matched layers for transient elastodynamics of unbounded domains. Numerical Meth Engineering **59**, 1039–1074 (2004). https://doi.org/10.1002/nme.896
20. D.V. Jones, M. Petyt. Ground vibration in the vicinity of a strip load: an elastic layer on a rigid foundation. J. Sound Vib. **152**, 501–515 (1992). https://doi.org/10.1016/0022-460X(92)90483-E
21. J. Wolf. Dynamic soil-structure interaction. (Prentice Hall, New Jersey, 1985)
22. Y.B. Yang, H.H. Hung, D.W. Chang. Train-induced wave propagation in layered soils using finite/infinite element simulation. Soil Dyn. Earthquake Eng. **23**, 263–278 (2003). https://doi.org/10.1016/S0267-7261(03)00003-4
23. A. El Kacimi, P.K. Woodward, O. Laghrouche, et al. Time domain 3D finite element modelling of train-induced vibration at high speed. Comput. Struct. **118**, 66–73 (2013). https://doi.org/10.1016/j.compstruc.2012.07.011
24. G. Kouroussis, D.P. Connolly, O. Verlinden. Railway-induced ground vibrations – a review of vehicle effects. Int. J. Rail Transp. **2**, 69–110 (2014). https://doi.org/10.1080/23248378.2014.897791
25. Livermore Software Technology Corporation (LSTC). LS-DYNA Keyword User's Manual, Volume I, Livermore, CA, USA, (2023)